The Formation of Black Patina on Copper in Humid Air Containing Traces of SO_2

Helena Strandberg* and Lars-Gunnar Johansson**

Department of Inorganic Chemistry, University of Göteborg, S-412 96 Göteborg, Sweden

ABSTRACT

The formation of a black patina on copper in humid air containing traces of SO_2 was investigated using on-line analysis of SO_2 and corrosion product characterization (x-ray photoelectron spectroscopy, Fourier transform infrared absorption spectroscopy, x-ray diffraction, and quantitative analysis of sulfite). In humid air (>75% RH) with 4 to 69 ppb SO_2, a dull black cuprite patina (200 to 300 nm thick) formed after 20 h exposure. However, when concentrations of SO_2 were higher, copper remained shiny, as did samples exposed at low humidity. Sulfate was the dominant sulfur species on shiny as well as on black samples. At high SO_2 concentrations copper is suggested to be passivated by a layer of chemisorbed sulfite on the thin air-formed oxide film, while at low concentrations the film breaks down. Corrosion mechanisms are suggested for this active/passive transition on the copper surface. The formation of cuprite on the black samples resulted in a high corrosion rate, and an inverse correlation between SO_2 concentration and corrosion was found. These results are in agreement with field studies on outdoor copper and bronze where the formation of a black cuprite patina and a high corrosion rate is observed in environments with low levels of SO_2.

Introduction

Copper exposed outdoors gradually develops a patina. Thus, the bright luster of a copper surface shortly darkens to become brown, later turning dull black. The dark layer mainly consists of cuprite (Cu_2O), but traces of copper hydroxy sulfate and copper hydroxy chloride may also be present. With time, the amount of basic copper salts increases and the well-known green patina may develop.

The question whether a green or a black patina will form has been discussed in the literature. In the early work of Vernon[1] it was pointed out that the formation of green patina was inhibited in districts sufficiently remote from sea and town. Vernon reported that copper spires in a remote part of Switzerland were still bright, except for yellow to rosy red interference colors, after at least 30 years exposure. This was supported by Weil *et al.*[2,3] who claimed, studying historical records, that the greenish blue patina on bronze sculptures often only develops in the presence of antropogenic emissions of patinating substances. In a field investigation of copper and copper alloy coupons, Holm and Mattson[4,5] observed that copper exposed for 16 years in rural atmosphere still showed blackish shades. In urban and marine sites, where SO_2 and chloride levels were higher and corrosion faster, appreciable signs of green patina were observed after 6 to 7 years.

It is known that SO_2 in the atmosphere accelerates the corrosion rate of several metals. In the case of copper corrosion, however, the situation is somewhat unclear. Results from field exposures in Sweden and Czechoslovakia[6,7] were interpreted to indicate SO_2 as a decisive factor influencing corrosion. However, the correlation between dose and response was better for zinc and steel than for copper. Henriksen and Fossestøl[8] carried out field exposures of copper in an environment in Norway containing SO_2 but only minor amounts of other pollutants. Their investigation showed SO_2 to be of minor importance to copper corrosion. The authors considered that the correlation between SO_2 concentration and copper corrosion rate found at other sites was caused by the presence of NO_2. The Norwegian study is supported by Tidblad and Leygraf[9,10] who found no correlation between weight increase and SO_2 concentration for copper. In environments with low levels of pollutants, a high weight gain was observed and Cu_2O was identified as the major corrosion product. These results are consistent with the surprisingly high corrosion rates found by Stöckle *et al.*[11] in rural areas after 1 year of exposure. After the second year the rate decreased, however. Further investigations in rural atmospheres by Odnevall and Leygraf[12] showed a rapid Cu_2O formation on copper during the first days of exposure, and the oxide layer achieved an average thickness of 100 to 150 nm. In other field exposures[13] at the Royal Castle in Stockholm, Sweden, the metal loss of copper was shown to be lowest in sites where the corrosion of zinc and steel was highest.

Several laboratory studies under controlled conditions have been performed to address the influence of SO_2 on copper corrosion.[14-27] Many of these studies involve SO_2 concentrations far in excess of what is found in outdoor atmospheres, for example, the clean troposphere has concentrations in the range 1 to 10 ppb, and polluted air has 20 to 200 ppb.[28] Already in the 1930s Vernon[14] investigated the effect of very high concentrations (0.01 to 10%) of SO_2 on copper and demonstrated the importance of water for the corrosion process. Vernon proposed that SO_2 decreases the local anodic pH sufficiently to cause increased oxide dissolution and hence, increases the corrosion rate. Chawla and Payer,[17] studying the early stages of corrosion on copper by moist air containing 0.5% SO_2, reported that a mixture of Cu_2O and CuS was formed and suggested that SO_2 participates as a cathodic depolarizer forming dithionite ($S_2O_4^{2-}$). However, considering the equilibrium potentials of the reactions in question, this reaction is thermodynamically disallowed. Exposing copper to humid air containing 10 and 100 ppm SO_2, Ericsson and Sydberger[18] identified sulfite $[Cu(I)_2Cu(II)(SO_3)_2 \cdot 2H_2O]$ and sulfate $[CuSO_4 \cdot 5H_2O]$ as the only crystalline corrosion products formed.

In the last decades, laboratory experiments have been performed with SO_2 in the ppb range. Abbott[19] first conducted experiments in this low concentration range to show the effects of mixtures of industrial air pollutants. Rice *et al.*[20] later reported on the corrosion rate of copper. In agreement with earlier field studies, they concluded that a correlation exists between SO_2 concentration and copper corrosion for atmospheres containing only SO_2 and for SO_2 in a mixture of corrosive trace gases. Eriksson *et al.*[22] studied the atmospheric corrosion of copper and reported that a combination of SO_2 and NO_2 produced a synergistic effect. The kinetics of the atmospheric corrosion of copper in humid air containing ppb levels of SO_2 was studied by Persson and Leygraf[23-25] using Fourier transform infrared absorption spectroscopy (FTIRAS). Rickett and Payer[26] used x-ray photoelectron spectroscopy (XPS) and coulometric reduction for investigations of the tarnish products caused by SO_2 and NO_2, and Song *et al.*[27] used *in situ* x-ray absorption fine structure (XAFS) measurements of the sulfur-containing species formed by SO_2.

In the reviewed laboratory studies, data on weight gain, metal loss, and the composition of the corrosion products

* Electrochemical Society Student Member.
** Electrochemical Society Active Member.

are reported, while little information is presented concerning the visual appearance of the samples. In an earlier study we reported on copper exposed to 500 ppb SO_2 at 70 and 90% relative humidity (RH).[22] In that study the appearance of the copper coupons was not changed much after 4 weeks exposure. The plates exposed at 90% RH had a darker hue but still showed a metallic luster. However, small green crusts were visible using an optical microscope.

In later studies in this laboratory, involving lower levels of SO_2, a surprising phenomenon appeared. When polished copper plates were exposed for half a day to 69 ppb SO_2 or less at 90% RH, they often turned dull black due to the formation of cuprite (Cu_2O). On some occasions, however, they remained shiny. The formation of a black patina was found to depend on relative humidity, SO_2 concentration, and the pretreatment of the samples.

In this work the formation of a black patina on copper in SO_2-containing atmospheres is investigated. To our knowledge, this phenomenon has not been reported in earlier laboratory studies. On the basis of results from time-resolved trace-gas analysis and corrosion product characterization (XPS, FTIR, XRD, and quantitative analysis of sulfite), corrosion mechanisms are suggested.

Experimental

Sample material and preparation.—The reference material was oxygenous cold-rolled 1/2-hard copper sheet metal [1.25 mm ISO Cu fiberglass reinforced thermoplastic (Cu-FRTP[R])] with a minimum copper content of 99.85%. This material is in common use for roofing, facing, furnishings, light fittings, and tanks. Other copper sheet materials were also investigated, as well as different methods of preparation (Table I).

Plates of copper were cut to shape (40 × 25 mm) and a hole was drilled in each for suspending the sample by a nylon thread. The samples were polished in ethanol with SiC paper to 1000 mesh. The plates were then cleaned in 99.9% ethanol using ultrasonic agitation and rinsed before drying at room temperature. The final geometrical area was 20 cm^2. The samples were stored in a desiccator over silica gel (<1% RH) for 24 h before the start of the long-term corrosion experiments and for 1 h before the short-term deposition experiments. After exposure the samples were also stored dry in a desiccator.

Experimental setup.—The experiments were carried out using two different experimental setups. The apparatus for on-line SO_2 deposition experiments is depicted in Fig. 1, while the corrosion exposure system has been depicted in a previous work.[29] All equipment was made of glass and Teflon and was immersed in a water tank kept at 22.00 ± 0.03°C. The temperature in the room was kept at 23 to 25°C in order to avoid condensation in the parts of the system outside the water tank. The first part of the setup consisted of an air purification and drying system consisting of particle filters, filters for the absorption of gaseous pollutants, and a self-regenerating air drier based on alumina. The CO_2 content in the purified air was about 200 ppm. The clean and dry air passed into the apparatus by two routes. One air flow passed through the humidifier in which the air was saturated with water vapor at 22.00°C. The other air flow was used as a carrier for SO_2 which was added from thermostated permeation tubes containing the liquefied gas. The total gas flow and the relative humidity was controlled by mixing measured amounts of dry and humidified air.

SO_2 deposition studies.—In the apparatus for short-term (20 h) deposition experiments (Fig. 1), a continuous flow of SO_2 containing humidified gas passed through the reaction cell. The sample was suspended by a nylon string, the corrosive gas flowing parallel to the sample. At standard conditions the dimensions of the corrosion cell were d = 45 and l = 350 mm, and the gas flow rate 1 liter/min, resulting in a gas velocity of 10.5 mm/s. Flow conditions were laminar in the cell (Re ≈ 30). The standard gas composition was 90% RH and 69 ppb SO_2.

The SO_2 concentration in the gas emanating from the reaction cell was measured continuously using a fluorescence instrument (Environnement AF21M). The instrument had a time constant of 1 min and the sensitivity was 1 ppb. Inserting or removing the samples from the reaction cell resulted in a small dilution peak (5 to 10%) lasting about 2 min. Hence, the term "initial deposition of SO_2" refers to the deposition registered 4 min after closing the cell, when the influence of the opening of the cell was assumed to be nil.

The deposition rate and the deposition velocity were determined by comparing input and output concentrations of SO_2. The deposition rate (mol/m^2 s) is defined as the flux of SO_2 to the sample surface. The deposition velocity (m/s) is defined as the deposition rate divided by the concentration of SO_2 [the average of the input and output concentrations in the cell].[30]

Corrosion studies.—In the corrosion exposure system used for the 4 week studies, the corrosive humidified gas passed through eight parallel corrosion chambers, each with a volume of 0.4 liter and an inner diameter of 55 mm (Fig. 2, Ref. 29). Each sample was exposed in a chamber of its own. In order to get equal gas flow in all chambers, a multichannel solenoid valve distributed the gas sequentially among the exposure chambers, the whole gas flow passing each chamber in turn for 37.5 s. The gas flow rate was 1 liter/min, this being equal to a gas velocity of 7 mm/s each time a chamber was open. Flow conditions were laminar (Re ≈ 25).

Table I. The influence of sample material, pretreatment, and experimental conditions on the visual appearance of copper samples after exposure in 90% RH and 69 ppb SO_2 for 20 h.

Sample		Appearance	Sample	Appearance	Sample	Appearance
Material (content in w/o[a]):			Pretreatment:		Experimental conditions:	
ISO Cu-FRTP 1/2 Hard	Cu > 99.85	Black	Stored in desiccator 10 min to 24 h	Black	Flow rate 0.06 to 5 liter/min	Black
ISO Cu-DHP Hard	P: 0.015 to 0.040 Fe: 0.005	Black	Polished in water	Black	Flow rate 1 liter/min, gas velocity 1 to 24 mm/s (chamber d = 30 to 150 mm)	Black
ISO Cu-DHP Soft	P: 0.015 to 0.040 Fe: 0.005	Black	Stored in air at 90% RH for 3 days	Shiny	No gas flow	Shiny
ISO Cu-OF	Cu > 99.99 O < 0.0005	Black	Stored in laboratory air for 1 h	Small black dots	Flow rate 1 liter/min 37.5 s, followed by no gas flow 187.5 s	Shiny or small black dots
ISO CuAg0.1 (OF)	Cu-Ag > 99.99 Ag: 0.08 to 0.12 O < 0.0005	Black	Annealed 115°C, 5 h	Shiny		
Cu-foil m4N	Cu > 99.999	Black				
Repolished plates used in various experiments		Sometimes shiny				

[a] Weight percent.

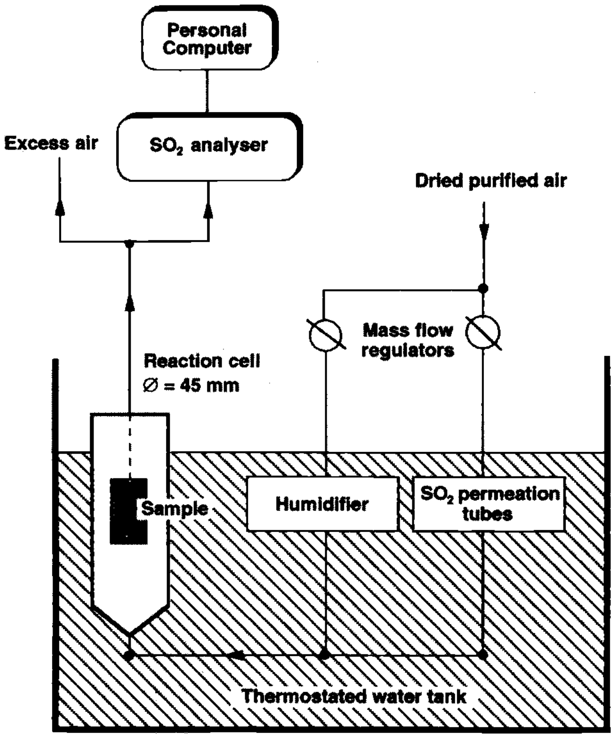

Fig. 1. Experimental setup for on-line studies of SO_2 deposition.

Grazing angle XRD.—For phase identification, x-ray powder diffraction (XRD) was used. Corroded plates were analyzed in a Siemens 5000D θ-θ diffractometer in Bragg-Brentano geometry using the grazing-incidence angle technique. Cu $K_{\alpha 1}$ radiation was used (λ = 1.54056 Å) and the incidence angle was 0.5°.

Specular FTIRAS.—IR spectra were obtained using FTIRAS. The instrument was a Perkin-Elmer 1800 Fourier transform infrared spectrometer. A specially developed sample holder for studies of metal surfaces was used, the unpolarized infrared beam striking the sample 80° from the normal.[31] Difference spectra were obtained at a resolution of 4 cm^{-1} using polished copper as reference.

Quantitative analysis for sulfite.—After the short-term SO_2-deposition studies, some samples were analyzed for sulfite. A three-necked round-bottomed flask made of glass containing 40 ml 1 *M* $HClO_4$(aq) replaced the corrosion chamber in Fig. 1. The exposed sample was immersed in the perchloric acid causing the following reactions

$$SO_3^{2-} + H^+ \rightarrow HSO_3^- \quad [1]$$

$$HSO_3^- + H^+ \rightarrow SO_2(aq) + H_2O \quad [2]$$

$$SO_2(aq) \rightarrow SO_2(g) \quad [3]$$

The SO_2(g) evolved was carried to the fluorescence SO_2 analyzer by a stream of purified air. Knowing the rate of air flow the amount of sulfite on the copper surface was calculated by integrating the output signal from the SO_2 analyzer. This analysis has a sensitivity of about 2×10^{-11} moles of SO_2. The reliability of the method was checked by adding known amounts of Na_2SO_3(s) to the acid, 100 ± 0.5% of the sulfite being recovered as SO_2(g).[22] The presence of metallic copper did not change this number appreciably. It may be noted that all sulfur-oxygen species with oxidation states below +VI evolve SO_2 upon immersion in acid.[32] However, as evidence was found only for sulfite (+IV) and sulfate (+VI) (see XRD, XPS, and FTIRAS) the evolution of SO_2 is considered to be due to sulfite.

XPS.—Surface layers of sample plates were analyzed (1 to 5 nm in depth) on a PHI 5500 XPS instrument. The monochromatic x-ray source Al K_α (1486.6 eV) was used at a total power dissipation of 350 W. The analyzed sample area was 0.5 mm^2 (d = 0.8 mm) at a take-off angle of 45°. Survey scans were performed from 0 to 1100 eV and 0 to 500 eV with a pass energy of 93.9 eV. For high-resolution information multiplex scans were performed with a pass energy of 23.5 eV and at a step size of 0.05 eV for S (2p) (158 to 178 eV), C (1s) (280 to 300 eV), O (1s) (525 to 545 eV), and Cu (2p) (924 to 954 eV). No smoothing routine was performed on background noise. All photoelectron peaks were normalized assuming the C (1s) peak from hydrocarbon contamination to be located at 284.8 eV. The separation of the two photoelectron peaks $2p_{1/2}$ and $2p_{3/2}$ of sulfur was determined by analyzing the spectrum of pyrite (FeS_2) and was found to be 1.2 eV. The $2p_{1/2}$:$2p_{3/2}$ area relation was taken to be 1:2, corresponding to the electron population of the respective levels. The full width at half maximum (FWHM) of the sulfur peaks in the pyrite spectrum (0.95 eV) was used in the deconvolution procedure.

Results

Visual appearance of copper samples.—The dark opaque areas formed on copper in some of the experiments are designated "black areas" in this paper. However, the color was actually brownish black, especially after drying, and resembled the dark patina developing on outdoor copper. Occasionally, black samples had a bluish hue, and in the case of very low concentrations of SO_2 the black areas appeared grayish. The appearance of the sample plates after exposure varied in the series of experiments. Some samples turned dull black almost all over the surface. However, edges and the area close to the hole used for suspension tended to remain shiny. Sometimes only parts of the sample turned black while in other cases small dark spots appeared on an otherwise shiny surface. Using optical microscopy, small pits were detected at the center of the black spots. Some samples did not change appearance, retaining their metallic luster throughout the experiment.

Concentration and RH dependence.—Figure 2 illustrates the occurrence of black patina on copper in SO_2-containing atmospheres depending on relative humidity and SO_2 concentration. The polished copper samples retain their metallic luster when humidity is below 75% RH, irrespective of the SO_2 concentration. When the relative humidity is about 80% and SO_2 concentration is low (below about 500 ppb), small dark spots appear on the copper surface. At even higher humidity and low SO_2 concentration copper tends to become black all over the sur-

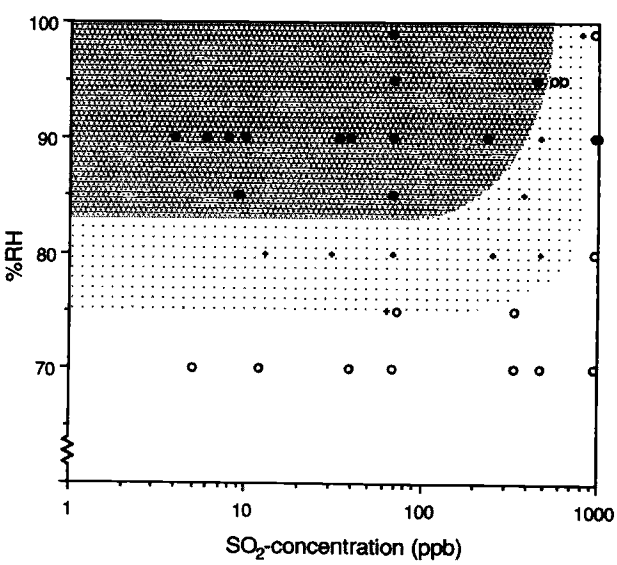

Fig. 2. Visual appearance of copper samples after 20 h exposure in atmospheres of various RH and SO_2 concentrations; (●), (+), and (○) indicate black, spotted, and shiny samples, respectively.

Table II. Binding energies (eV) for some reference compounds using XPS.

Compound	S ($2p_{3/2}$)	O (1s)	Cu ($2p_{2/3}$)	Ref.
$Na_2S_2O_3$	161.7, 167.7			36
	162.4, 167.5			37
CuS	162.2			38
Cu_2S	162.0			38
S_8	164.0			36
$Na_2S_2O_4$	166.6			37
Na_2SO_3	166.5			36
"Copper sulfite"	167.1 to 167.2		935.5	23
$Cu(I)_2Cu(II)(SO_3)_2 \cdot 2H_2O$	168.6	532.8	934.0, 937.2	39
			935.6	40
Brochantite Antlerite $Cu_{2.5}(OH)_3SO_4 \cdot 2H_2O$	168.4 to 168.7	531.4 to 531.8	934.7 to 934.8	41
$CuSO_4$	168.9,[42] 169.2[38]	532.0[38]	935.3	42, 38
Copper sulfate	169.0-1,[23] 168.2[43]			23, 43,
CuO		529.7	933.9	42
Cu_2O		530.2	932.5	42
$Cu(OH)_2$		531.3,[42] 531.5[44]	934.7	42, 44
Chemisorbed water		532.5,[42] 533.3[44]		42, 44
Cu^{2+}			944, 963	26

All photoelectron peaks are normalized assuming the C (1s) peak from hydrocarbon contamination to be located at 284.8 eV. Small superscript numbers refer to references listed in last column.

face. However, when SO_2 concentration is high (about 1 ppm) the copper samples remain shiny at all humidities. In humid air with no SO_2 present copper also remains shiny.

Material dependence.—Various types of copper sheet material were exposed to the standard conditions (90% RH, 69 ppb SO_2, etc.) all turning blackish (Table I). Thus, no influence of sample composition or cold work upon the formation of the black patina was found.

Pretreatment dependence.—The storage time between polishing and exposure did not influence the appearance of samples after exposure as long as they were stored dry in a desiccator (Table I). However, when plates were stored at 90% RH for 24 h or in the laboratory air, they tended to remain shiny when exposed to the standard conditions (90% RH, 69 ppb SO_2, etc.) probably due to the formation of a persisting surface film. A polished sample that was annealed in air at 115°C for 5 h prior to exposure also remained shiny. Polishing in water instead of ethanol had no influence on the appearance after exposure.

Air speed dependence.—Samples exposed to a continuous flow of air (Fig. 1) with 69 ppb SO_2 at 90% RH turned black irrespective of the gas velocity in the cell in the range 1 to 24 mm/s. However, samples exposed to the same gas composition in the eight-chamber corrosion exposure system, featuring a pulsed flow, showed somewhat less propensity to develop the black patina. No systematic investigation of the formation of black patina was made using the eight-chamber exposure system.

Qualitative analysis of corrosion products.—Grazing angle XRD analysis of a dull black surface (after 20 h exposure in 69 ppb SO_2 at 90% RH) showed the presence of cuprite, while no crystalline corrosion products could be detected on a shiny area. On analyzing samples exposed to 6, 69, and 976 ppb SO_2 with FTIRAS, two peaks were found at 978 and 1108 cm^{-1}, indicating the presence of sulfite and sulfate.

XPS studies were performed on polished unexposed copper and on an exposed copper sample (69 ppb SO_2 at 90% RH for 20 h) exhibiting black as well as shiny areas. Figure 3 depicts the copper, oxygen, and sulfur XPS, respectively, for the three sample areas. Table II lists the binding energies for some reference compounds and Table III the photoelectron peaks and assignments for the different sample areas. The XPS results (Fig. 3, Table III) indi-

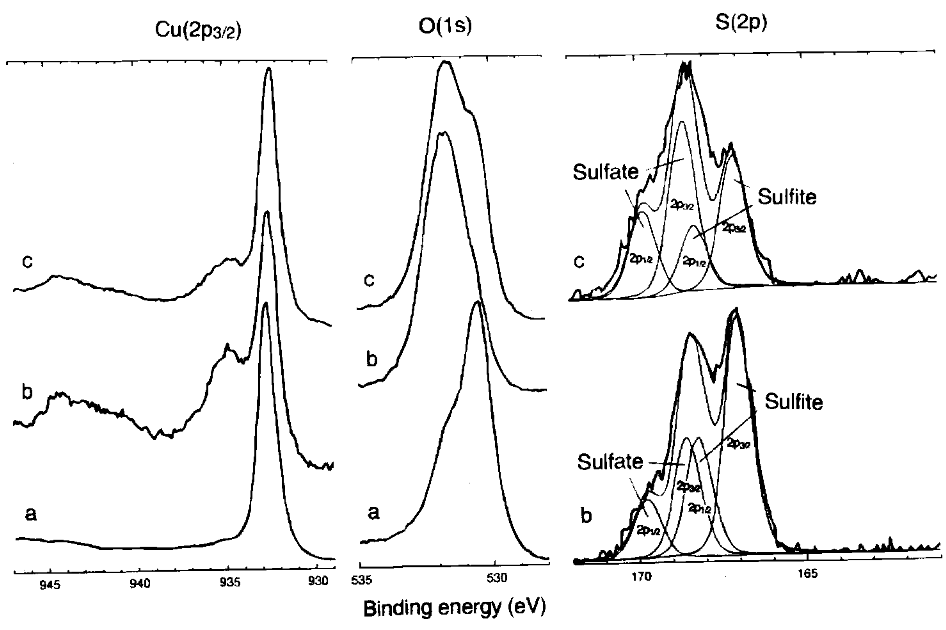

Fig. 3. Copper ($2p_{3/2}$), oxygen (1s), and sulfur (2p) XPS of (a) polished unexposed copper sample, (b) a shiny area of a copper sample exposed to 69 ppb SO_2 at 90% RH, and (c) a black area of a copper sample exposed to 69 ppb SO_2 at 90% RH.

Table III. Film composition of sample areas analyzed using XPS. Binding energies in eV.

Sample area	S ($2p_{3/2}$)	O (1s)	Cu ($2p_{3/2}$)	C (1s)	Assignment
Unexposed sample area		530.5	932.6		Cu_2O
		531.6			Surface hydroxide
				288.3	CO_3^{2-} or carboxylate
Shiny area exposed to 69 ppb SO_2 at 90% RH for 20 h			932.6		Cu_2O
			934.8		Cu^{2+}
			944		Cu^{2+}
	167.0				Sulfite
	168.5				Sulfate
		531.7			Surface hydroxide, sulfite, or sulfate
				288.5	CO_3^{2-} or carboxylate
Black area exposed to 69 ppb SO_2 at 90% RH for 20 h		530.5	932.4		Cu_2O
			934.8		Cu^{2+}
			944		Cu^{2+}
	167.0				Sulfite
	168.5				Sulfate
		531.5			Surface hydroxide, sulfite, or sulfate
				288.5	CO_3^{2-} or carboxylate

All photoelectron peaks are normalized assuming the C (1s) peak from hydrocarbon contamination to be located at 284.8 eV.

cate the presence of cuprite (530.5 eV) and possibly surface hydroxide (531.6 eV) on the unexposed sample surface. The presence of a peak at 934.8 eV and a shake-up band at 944 eV on the exposed sample indicates Cu^{2+} to be present on shiny as well as on black areas. In accordance with the XRD results the black area gives stronger indications for cuprite (530.5 eV) than the shiny area. Sulfite and sulfate is indicated by two peaks for S ($2p_{3/2}$) at 167.0 and 168.5 eV on the exposed sample areas, the S(IV)/S(VI) ratio being higher for the shiny area. Moreover, trace amounts of carbonate or carboxylates (288.3 to 288.5 eV) were detected on exposed as well as on unexposed samples (Table III).

Deposition studies.—The deposition curves in the different experiments varied depending on the extent of black area formed, the rate of blackening, and when blackening was initiated. Representative runs for black and shiny samples (out of 20 runs) are shown in Fig. 4. The deposition of SO_2 on polished copper is initially fast but rapidly slows down. A dry copper sample stored in a desiccator causes a sharp initial deposition peak when placed in the reaction cell. However, for samples stored in clean humid air before exposure the initial peak is less pronounced. The total amount of sulfur accumulated after 20 h is about the same in both cases. At 90% RH and 69 ppb SO_2, the deposition of SO_2 passes through a minimum after a few hours. Simultaneously, a dense pattern of small reddish brown dots appears on parts of the sample surface. The pattern of dots quickly develops to become even denser, and in an hour, continuous dull dark areas are observed. The deposition of SO_2 on the sample increases as the dark areas expands all over the surface. When the lateral growth of the dark areas ceases, the deposition of SO_2 again decreases. After 20 h exposure the sample appears black. Under conditions of lower humidity, *e.g.*, 70% RH or at higher concentrations of SO_2, the black patina does not form and the deposition decreases continuously until steady state is reached (Fig. 4).

Quantitative study of SO_2 deposition.—The initial rate of SO_2 deposition in humid air (70 to 99% RH) was found to be proportional to the concentration of SO_2 and independent of RH. Based on 20 independent runs, 32% of the SO_2 passing the sample (the scatter being ±7%) was deposited initially, corresponding to a deposition velocity of about 3.2×10^{-3} m/s. At 0% RH the initial deposition velocity was less (1.1×10^{-3} m/s). A glass sample ($0.1 \times 2.5 \times 4$ cm) covered with a thin layer of NaOH was exposed to determine the mass transfer-limited deposition of SO_2 on a sample. The deposition on NaOH was found to be about 32% (the scatter being ±5%). This comparison demonstrates that a clean copper surface initially acts as an ideal absorber for SO_2 in humid air.

The deposition rate of SO_2 after 20 h exposure is strongly RH dependent (Fig. 5). The deposition velocity, depicted in Fig. 6, is very high at low SO_2 concentration but sharply

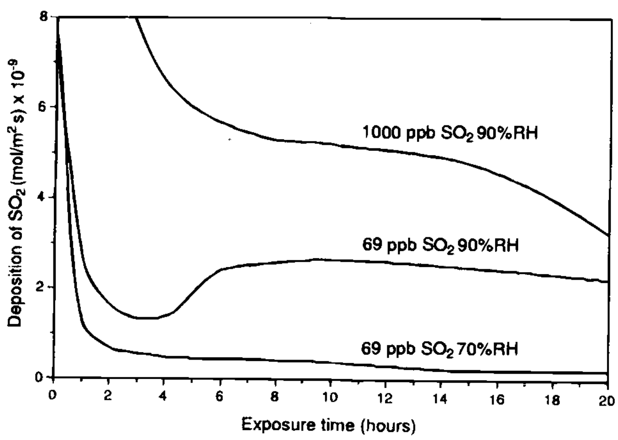

Fig. 4. SO_2 deposition rate as a function of time for samples exposed to 69 ppb SO_2 at 70% RH, 69 ppb SO_2 at 90% RH, and 1000 ppb SO_2 at 90% RH, respectively.

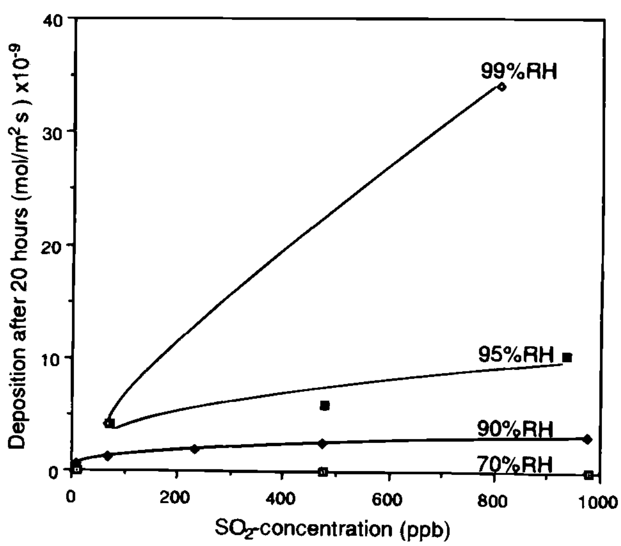

Fig. 5. SO_2 deposition rate after 20 h exposure. The lines are guides to the eye.

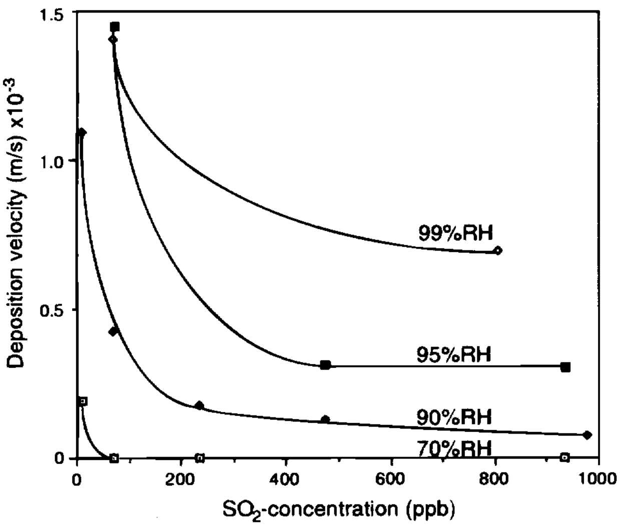

Fig. 6. Deposition velocity for SO_2 on copper after 20 h exposure. For an ideal absorber, the deposition velocity is 3.2×10^{-3} m/s. The lines are guides to the eye.

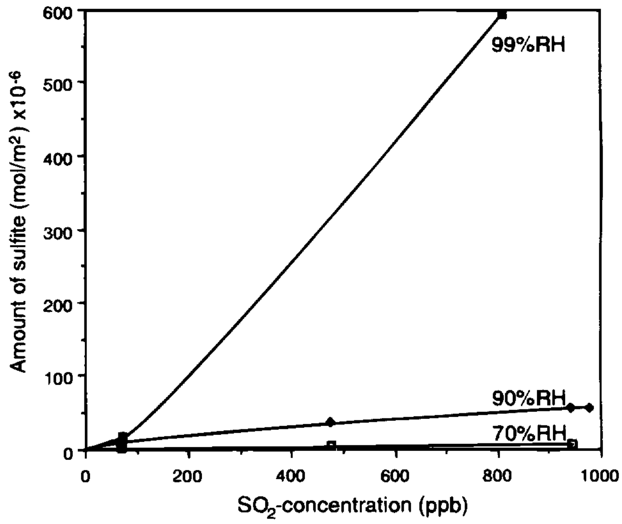

Fig. 7. The amount of sulfite [S(IV)] on copper after 20 h exposure determined by quantitative analysis. The lines are guides to the eye.

decreases with higher concentration. The total amount of sulfur accumulated is small at 70% RH (Table IV). At 90 and 99% RH, the amount is higher and increases with SO_2 concentration.

Quantitative analysis of S(IV) on the copper surface.—The amount of sulfite on the copper surface was determined by quantitative analysis and is depicted in Fig. 7. At 70% RH the amount of sulfite is low. At higher humidity (90% RH or more) the amount of sulfite is greater and increases with the concentration of SO_2. The fraction of the sulfur accumulated which is present in the sulfite [S(IV)] state increases with SO_2 concentration and humidity, as indicated in Table IV.

The sulfur not determined as sulfite (see Experimental) may be sulfide, elemental sulfur, or sulfate. As no evidence was found for sulfide or elemental sulfur (Fig. 3), we assume that the total sulfur accumulated (Table IV) is sulfite or sulfate. However, we cannot rule out the possibility that traces of other sulfur species are present. Table IV shows that sulfite never dominates, consequently sulfate is considered to always be the most abundant species.

Samples exposed to clean humid air immediately after exposure to SO_2-containing air, desorbed SO_2. The desorption of SO_2 at 90% RH, after 20 h exposure to SO_2, corresponded to 10 to 20% of the total amount of S(IV) present on the surface. However, in dry clean air there was no desorption at all. Shiny copper plates exposed to high concentrations of SO_2 desorbed SO_2 and gradually turned black during prolonged exposure to SO_2-free humid air.

Weight gain studies.—The weight gains were recorded after storing the samples in a desiccator (<1% RH) for at least 1 week. It was related to the extent of the black areas

Table IV. Total amount of sulfur accumulated during exposure (S_{tot}) and the ratio sulfite/total sulfur ($S(IV)/S_{tot}$).

Exposure time	RH	SO_2 concentration (ppb)	S_{tot} (mol/m^2) $\times 10^{-6}$	$S(IV)/S_{tot}$
20 h	70%	12	35	0.7%
20 h		69	43	4.8%
20 h		476	60	4.7%
20 h		958	67	10.5%
20 h	90%	10	60	1.8%
20 h		69	110	4.5%
20 h		476	318	11.3%
20 h		978	440	13.3%
40 min		69	12	9.0%
20 h	99%	69	264	7.0%
20 h		807	2170	27.5%

on the samples. For samples exposed to 69 ppb SO_2 at 90% RH, the weight gain was 15 to 20 μg/(cm^2 of black area) after 20 h and 30 to 45 μg/(cm^2 of black area) after 4 weeks, while for shiny plates it was not measurable (<2 μg/cm^2 after 20 h exposure). The weight gain of the black samples (about 300 μg/sample after 20 h when A = 20 cm^2) was mainly due to the uptake of oxygen by the metal, as the deposited amount of SO_2 only corresponds to about 14 μg/sample. Assuming only cuprite was formed, the thickness of the black layer is calculated to be 230 to 300 nm after 20 h. The higher weight gain found when samples were exposed in the same atmosphere for 4 weeks may be ascribed to a thicker black layer of cuprite and to the uptake of more SO_2. Samples exposed to 484 ppb at 90% RH for 4 weeks exhibited only small spots of black cuprite.

Discussion

The formation of a dull black cuprite patina reported in this study has been shown to depend on relative humidity and SO_2 concentration as depicted in Fig. 2. This observation can be explained in terms of an active/passive transition on the copper surface. The various ways that SO_2 may interact with the surface and the subsequent breakdown of the protective film are described by reactions 4 to 16 and are schematically illustrated in Fig. 8.

Adsorption of SO_2

$$\equiv\overset{\mathrm{I}}{\mathrm{Cu}}\text{-OH(ads)} + SO_2(g) \rightarrow \equiv\overset{\mathrm{I}}{\mathrm{Cu}}\text{-}SO_3^-\text{(ads)} + H^+ \quad [4]$$

Formation of soluble sulfite

$$\equiv\overset{\mathrm{I}}{\mathrm{Cu}}\text{-}SO_3^-\text{(ads)} \leftrightarrow Cu^+ + SO_3^{2-} \quad [5]$$

$$\equiv\overset{\mathrm{I}}{\mathrm{Cu}}\text{-}SO_3^-\text{(ads)} + H_2O \leftrightarrow \equiv\overset{\mathrm{I}}{\mathrm{Cu}}\text{-OH(ads)} + SO_3^{2-} + H^+ \quad [6]$$

Desorption of SO_2

$$SO_3^{2-} + 2H^+ \leftrightarrow H_2O + SO_2(g) \quad [7]$$

Formation of solid sulfite

$$Cu^+ + SO_3^{2-} \leftrightarrow \text{copper sulfite(s)} \quad [8]$$

Oxidation of sulfite

$$\equiv\overset{\mathrm{I}}{\mathrm{Cu}}\text{-}SO_3^-\text{(ads)} + 1/2\ O_2 \rightarrow \equiv\overset{\mathrm{I}}{\mathrm{Cu}}\text{-}SO_4^-\text{(ads)} \quad [9]$$

$$SO_3^{2-} + 1/2\ O_2 \rightarrow SO_4^{2-} \quad [10]$$

Formation of soluble sulfate

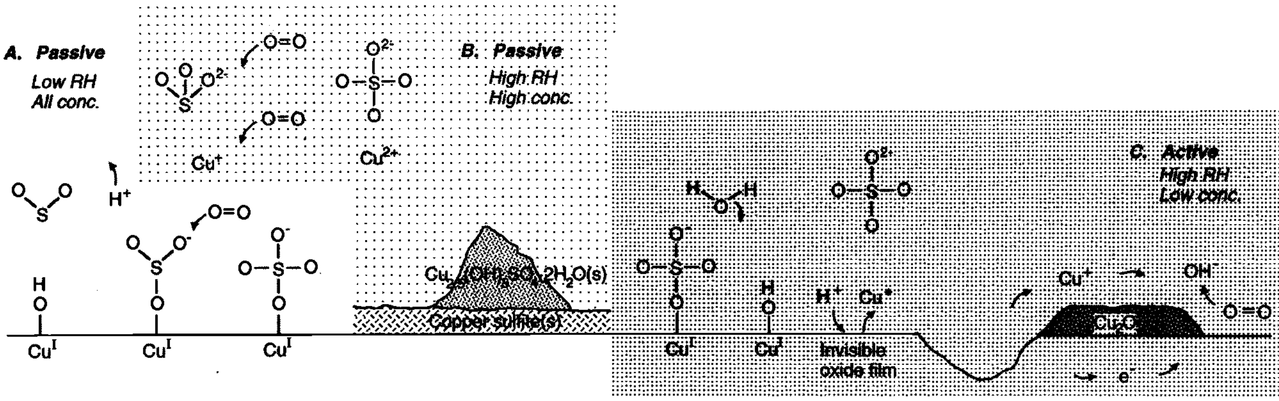

Fig. 8. A schematic view of the interaction of SO_2 with a copper surface in humid air. (A) The passive surface at low RH, (A + B) the passive surface at high RH and high concentration, and (A + B + C) the breakdown of the thin invisible oxide film at high RH and low concentration and the subsequent active corrosion.

$$\equiv\overset{I}{Cu}\text{-}SO_4^-(ads) + H_2O \rightarrow \equiv\overset{I}{Cu}\text{-}OH(ads) + SO_4^{2-} + H^+ \quad [11]$$

Oxidation of Cu

$$Cu^+ + 1/4\ O_2(g) + H^+ \rightarrow Cu^{2+} + 1/2H_2O \quad [12]$$

$$Cu(s) \leftrightarrow Cu^+ + e^- \quad [13]$$

Reduction of O_2

$$1/2\ O_2 + 2H^+ + 2e^- \rightarrow H_2O \quad [14]$$

Formation of solid sulfate

$$Cu^{2+} + SO_4^{2-} \rightarrow Cu_{2.5}(OH)_3SO_4 \cdot 2H_2O(s) \quad [15]$$

Dissolution of the passive film

$$Cu_2O(s) + 2H^+ \leftrightarrow 2Cu^+ + H_2O \quad [16]$$

Interaction of SO_2 with the surface.—The polished copper surface is covered by an invisible air-formed film of copper(I) oxide that appears to be hydroxylated according to XPS. In humid air the initial deposition rate of SO_2 on copper is independent of RH while it is somewhat lower at 0% RH. This indicates that the surface coverage of hydroxyl groups approaches unity in humid air while the surface is only partly hydroxylated at 0% RH. The deposition of SO_2 is initially very fast (Fig. 4), rapidly slowing down as the surface sites become occupied with adsorbed sulfite (reaction 4). However, the deposition never ceases completely and it is suggested that this is caused by the conversion of adsorbed sulfite to soluble species. This would create new adsorption sites where SO_2 can subsequently adsorb.

Copper initially behaves as an ideal absorber for SO_2, the deposition rate being equal to the mass transfer-limited value. However, Persson and Leygraf[25] reported the initial deposition on copper in a similar environment to be only a fraction of the mass transfer-limited value. One reason for this apparent contradiction may be that they consider the deposition of SO_2 on the surface to be proportional to the intensity of an IR absorption band assigned to sulfite. However, in this study we find that sulfate is invariably the dominant sulfur species throughout the exposures.

The presence of sulfite on copper exposed to ppb levels of SO_2 has been reported by Eriksson *et al.*[22] using quantitative analysis, as well as by Persson and Leygraf,[23-25] using FTIRAS and x-ray photoelecspectroscopy and is confirmed by the present study. The first step in the deposition of SO_2 on a clean copper surface is proposed to correspond to the formation of adsorbed sulfite on the hydroxylated oxide film (reaction 4). Sulfite, being an ambiodentate ion, may coordinate either through sulfur or oxygen.[25] The reaction of SO_2 initially results in O-coordinated surface sulfite which may later reorganize to form a S–Cu bond. The amount of sulfite found by quantitative analysis at 70% RH (Fig. 7) corresponds to less than one monolayer (8.6×10^{-6} mol/m^2)[25] and is suggested to be mainly chemisorbed sulfite occupying all available surface sites. The observation that exposed copper samples desorb SO_2(g) in humid air but not in dry air implies that desorption involves an aqueous film. An exchange is proposed to occur between chemisorbed sulfite and sulfite species dissolved in the aqueous surface layer (reactions 5 and 6), followed by the release of SO_2 to the gas phase according to reaction 7. Figure 7 shows that large amounts of sulfite, corresponding to substantially more than a monolayer, form only when RH ≥ 90% and SO_2 concentration is high. This implies that the precipitation of solid copper sulfite (reaction 8) is possible only at high humidity when the aqueous surface film becomes an efficient electrolyte.

Previous investigators[22,23,25] have reported the presence of sulfate on copper exposed to humid air containing traces of SO_2. In this study most of the sulfur accumulated on the surface was found to be sulfate (Table IV). This implies that sulfite oxidizes to sulfate by reactions involving either adsorbed sulfite (reaction 9), or sulfite species in solution (reaction 10). As sulfate dominates also at 70% RH where the amount of dissolved sulfite species is low, one may conclude that the oxidation of adsorbed sulfite (reaction 9) is rather fast. In aqueous solution, copper(I) sulfite complexes tend to be much stronger than the sulfate complexes of Cu(I) and Cu(II).[33] It is expected that the same is true for the corresponding surface complexes formed on the thin oxide film. This suggests that whereas sulfite adsorbs quite strongly to the oxide film, oxidation to sulfate (reaction 9) leads to the detachment of sulfate and the regeneration of an adsorption site on the surface (reaction 11).

Analyzing exposed samples with XPS, the formation of divalent copper was observed. Cu(II) may form by oxidation of Cu(I) species on the surface, in the aqueous layer (reaction 12) or by disproportionation of Cu^+. It is suggested that divalent copper in the surface electrolyte precipitates as copper hydroxysulfate (reaction 15), initially in the form of $Cu_{2.5}(OH)_3SO_4 \cdot 2H_2O$,[34] as reported previously.[22]

Copper exposed to humid air with ppb levels of SO_2 has been reported to form a corrosion product with an outer layer containing sulfur-oxygen species and an inner layer containing copper sulfide.[26] The inner, sulfide layer was only detected after ion etching, however. In the present study XPS measurements gave no indication of sulfur in oxidation states below +IV (Fig. 3); however, no ion etching was performed. The reason for not using ion etching was that zinc sulfite tends to decompose upon ion etching (Ar + ion gun, 4 kV, 1 min), forming a mixture of sulfide and sulfate.[35] The detection of a sulfide peak in the XPS spectrum after ion etching therefore does not prove the presence of sulfide in the undisturbed corrosion product.

Passivation and breakdown of the passive film.—In atmospheres containing high levels of SO_2, copper remains shiny, whereas low SO_2 concentration leads to a sudden transition to active corrosion. It is therefore concluded that high concentrations of SO_2 passivate copper.

At low humidity the tendency for adsorbed sulfite to form species in solution (reactions 5 and 6) is slight, which implies that the conversion to solid sulfite (reaction 8) and the formation of sulfate (reaction 9 and 10) is slow. Moreover, the hydroxyl groups formed in reaction 6 are expected to react rapidly with SO_2, forming new adsorbed sulfite (reaction 4). This leads to a high stability of the adsorbed sulfite, explaining the very low rate of SO_2 deposition at steady state (Fig. 5). It is proposed that the metal surface never enters the active state because it is protected by the adsorbed sulfite film (illustrated in Fig. 8A). This would correspond to the part of Fig. 2 where RH is below 75% and where copper retains its metallic luster throughout exposure.

When humidity is higher, the exchange between adsorbed sulfite and species in solution (reactions 5 and 6) is faster. This explains the higher rate of SO_2 deposition (Fig. 5), the formation of large amounts of solid sulfite (Fig. 7), and the faster oxidation to sulfate (Table IV) on the copper surface. A higher SO_2 concentration is needed to ensure the integrity of the protective chemisorbed sulfite layer (reaction 4) and maintain copper in the passive state. It is possible that the formation of solid copper sulfite further increases the tendency to passivate copper. These conditions correspond to the upper right corner of Fig. 2 (illustrated in Fig. 8B).

When SO_2 concentration is low and humidity high (upper left part of Fig. 2), copper enters into the active state (illustrated in Fig. 8C). It is proposed that the transition to the active state occurs because the adsorbed sulfite layer is destroyed. This is due to the formation of soluble sulfite species (reactions 5 and 6) and to the oxidation of the sulfite followed by the detachment of sulfate (reactions 9 and 11). Once this happens the thin oxide film faces an aggressive environment, the surface electrolyte exhibiting low pH and high conductivity, and is dissolved by the acid (reaction 16). Consequently, the anodic dissolution of copper starts (reaction 13), forming a pit. In the corresponding cathodic reaction atmospheric oxygen is reduced on the thin oxide film (reaction 14). Subsequently, cuprite precipitates close to the pit (reaction 16). As the cuprite layer grows in thickness (to about 200 nm) its resistance increases, pushing the cathodic area to the surroundings of the precipitation rim. Cuprous ions migrate in the surface electrolyte from the pit toward the cathodic areas, precipitating more cuprite. This transition to the active state is observed as many small dark dots appearing on the surface. The pattern of dots rapidly becomes denser, eventually forming a continuous black cuprite film. Simultaneously, as the dark dots appear on the surface the deposition of SO_2 starts to increase (Fig. 4). The increased uptake of SO_2 is suggested to be caused by the formation of cuprite, providing new adsorption sites, and by the increase of the surface electrolyte pH at the cathodic areas. SO_2 deposition continues to increase as the black areas develop but slows down again once the whole sample has turned black.

Exposing copper to RH/pSO_2 conditions corresponding to the intermediate region between the active and passive areas (Fig. 2) results in the formation of millimeter size black spots on the surface. The spots, mainly consisting of Cu_2O, form in the same way as the continuous black patina. However, in this case only a small fraction of the surface is affected. The spots exhibit microscopic pits at the center, presumably corresponding to the location of the anodic sites.

Laboratory investigations in relation to field studies.—It is evident that copper exposed to the outdoor atmosphere can develop a patina of similar appearance and composition as found in the present investigation.[4,5,10-12] In rural areas copper has been reported to form stains initially and later to turn black, cuprite (Cu_2O) being the main corrosion product. The reason why this laboratory study was able to mimic this characteristic patina may be that it was performed at sufficiently low SO_2 concentration and high relative humidity to avoid passivating the copper surface.

As noted in the Introduction, some recent field studies have reported copper to exhibit surprisingly high corrosion rates in rural atmospheres.[10-12] Thus, cuprite has been found to be abundant on test sites with low levels of pollutants. Neither has a clear correlation between SO_2 concentration and copper corrosion been found in outdoor exposures.[6-9] These observations have been suggested to be due to the synergistic influence of other pollutants on the corrosion process, *i.e.*, NO_2 and O_3.[10] This study shows that very low levels of SO_2 by itself may transfer copper into an active corroding state, forming large amounts of cuprite. An inverse correlation between the concentration of SO_2 and the atmospheric corrosion of copper is observed in the absence of other pollutants. These observations may help to explain the findings in the field studies.

Conclusion

The formation of a black patina on outdoor copper and bronze has been reported in many field studies. This is the first report on this phenomenon from laboratory exposures of copper in air with traces of SO_2. In humid air (>75% RH) containing 4 to 69 ppb SO_2, a dull black cuprite (Cu_2O) patina forms after 20 h exposure. However, when the concentration of SO_2 is higher or humidity is lower copper remains shiny. There is no influence of metal composition or cold work upon the formation of black patina. However, the pretreatment is important.

These results are explained in terms of an active/passive transition on the copper surface. It is suggested that the passivating effect of SO_2 at high concentration is caused by the formation of a layer of protective chemisorbed sulfite on the thin invisible air-formed oxide film. At low concentrations and high humidity the adsorbed sulfite layer is destroyed due to the formation of soluble species and oxidation to sulfate. The thin oxide film is attacked by the acid surface electrolyte and an electrochemical corrosion process can start. Consequently copper is anodically dissolved, oxygen is cathodically reduced and cuprite is precipitated forming a dull black layer (200 to 300 nm thick). Sulfate is the dominant sulfur species on shiny as well as on black samples.

The growth of cuprite on the black samples causes a high corrosion rate at low SO_2 concentration, resulting in an inverse correlation between SO_2 concentration and corrosion. These results are in agreement with findings in field studies on outdoor copper and bronze where the formation of a black cuprite patina and a high corrosion rate is observed in environments with low levels of SO_2.

Acknowledgments

We express our gratitude to Urban Jelvestam and Dr. Ingemar Olefjord at the Department of Engineering Metals, Chalmers University of Technology, for their expertise in performing the XPS investigations. We also thank Outokumpu Copper for supplying the copper sheet material.

Manuscript submitted Nov. 27, 1995; revised manuscript received Sept. 25, 1996.

REFERENCES

1. W. H. J. Vernon, *J. Inst. met.*, **49**, 153 (1932).
2. P. D. Weil, AIC Preprints, San Francisco, CA, May 1980, p. 129 (1980).
3. P. D. Weil, P. Gaspar, L. Gulbransen, R. Lindberg, and D. Zimmerman, in *Science and Technology in the Service of Conservation*, IIC Preprints, Washington, DC, p. 130 (1982).
4. R. Holm and E. Mattson, *Atmospheric Corrosion of Metals*, ASTM STP 767, S. W. Dean, Jr. and E. C.

Rhea, Editors, p. 85, American Society for Testing and Materials, Philadelphia, PA (1982).
5. E. Mattsson and R. Holm, in *Atmospheric Corrosion*, W. H. Ailor, Editor, Chap. 24 (1982).
6. D. Knotkova, J. Gullman, P. Holler, and V. Kucera, *International Congress on Metallic Corrosion*, Toronto, Ontario, Canada, June 3-7, 1984, Vol. 3, p. 198, National Research Council of Canada (1984).
7. V. Kucera, D. Knotkova, J. Gullman, and P. Holler, *International Congress on Metal Corrosion*, Madras, India, Vol. 1, p. 167, Central Electrochemical Research Institute (1987).
8. J. Henriksen and B. Fossestøl, *11th Scandinavian Corrosion Congress*, Stavanger, Norway F-48 (1989).
9. J. Tidblad, C. Leygraf, and V. Kucera, *This Journal*, **138**, 3592 (1991).
10. J. Tidblad and C. Leygraf, *ibid.*, **142**, 749 (1995).
11. B. Stöckle, S. Fitz, M. Mach, G. Pöhlmann, and R. Snethlage, *Werkst. Korros.*, **44**, 48 (1993).
12. I. L. Odnevall and C. Leygraf, *This Journal*, **142**, 3682 (1995).
13. B. Rendahl, V. Kucera, P. Norberg, and C. Sjöström, in *Wet and Dry Deposition of Acidifying Air Pollutants. Effects on Building Materials*, Swedish Corrosion Institute, Report 1995: **3**, Stockholm (1995), Summary in English.
14. W. H. J. Vernon, *Trans. Faraday Soc.*, **27**, 255 (1931).
15. T. Sydberger and N-G. Vannerberg, *Corros. Sci.*, **12**, 775 (1972).
16. I. L. Rozenfeld, in *Atmospheric Corrosion of Metals*, E. C. Greco, Editor, p. 125, NACE, Houston, TX (1972).
17. S. K. Chawla and J. H. Payer, *This Journal*, **137**, 60 (1990).
18. R. Ericsson and T. Sydberger, *Werks. Korros.*, **28**, 755 (1977).
19. W. H. Abbott, *IEEE Trans. Parts, Hybrids, Pack.*, **PHP-10**, 24 (1974).
20. D. W. Rice, P. Peterson, E. B. Rigby, P. B. P. Phipps, R. J. Cappell, and R. Tremoureux, *This Journal*, **128**, 275 (1981).
21. J. Henriksen and A. Rode, *10th Scandinavian Corrosion Congress*, Stockholm, p. 39 (1986).
22. P. Eriksson, L.-G. Johansson, and H. Strandberg, *This Journal*, **140**, 53 (1993).
23. D. Persson and C. Leygraf, *ibid.*, **137**, 3163 (1990).
24. D. Persson and C. Leygraf, *ibid.*, **140**, 1256 (1993).
25. D. Persson and C. Leygraf, *ibid.*, **142**, 1459 (1995).
26. B. I. Rickett and J. H. Payer, *ibid.*, **142**, 3713 (1995).
27. I. Song, B. Rickett, P. Janavicius, J. H. Payer, and M. R. Antonio, *Nucl. Instrum. Meth. Phys. Res.*, **A360**, 634 (1995).
28. J. H. Seinfeld, *Atmospheric Chemistry and Physics of Air Pollution*, p. 37, John Wiley & Sons, Inc., New York (1986).
29. J.-E. Svensson and L.-G. Johansson, *This Journal*, **143**, 51 (1996).
30. F. W. Lipfert, *JAPCA*, **39**, 446 (1989).
31. J.-E. Svensson and L.-G. Johansson, in *Proceedings of the 12th International Corrosion Congress*, p. 662, NACE (1993).
32. G. Nickles, *Inorganic Sulphur Chemistry*, Elsevier Publishing company, Amsterdam (1968).
33. R. M. Smith and A. E. Martell, *Critical Stability Constants: Inorganic Complexes*, Vol. 4, Plenum Press, New York (1976).
34. H. Strandberg, V. Langer, and L.-G. Johansson, *Acta Chem. Scand.*, **49**, 5 (1995).
35. J.-E. Svensson, Private communication, 1995, Department of Inorganic Chemistry, University of Göteborg, S-41296 Göteborg, Sweden.
36. B. J. Lindberg, K. Hamrin, G. Johansson, U. Gelius, A. Fahlman, C. Nordling, and K. Siegbahn, *Physica Scripta*, **1**, 286 (1970).
37. K. M. Abraham and S. M. Chaudhri, *This Journal*, **133**, 1307 (1986).
38. C. Perrin, D. Simon, D. Mollimard, M. T. Bajard, P. Baillif, and J. Bardolle, *J. Chim. Phys.*, **81**, 39 (1984).
39. H. Rupp and U. Weser, *Bioinorg. Chem.*, **6**, 45 (1976).
40. P. Brant and Q. Fernando, *J. Inorg. Nucl. Chem.*, **40**, 235 (1978).
41. H. Strandberg and L.-G. Johansson, Unpublished results.
42. S. K. Chawla, N. Sankarraman, and J. H. Payer, *J. Electron Spectrosc. Relat. Phenom.*, **61**, 1 (1992).
43. S. Zakipour and C. Leygraf, *This Journal*, **133**, 21 (1986).
44. C. Au, J. Breza, and M. W. Roberts, *Chem. Phys. Lett.*, **66**, 340 (1979).